Band Stop Filter with a Synthetic Inductor with Series Resistance and a Real Operational Amplifier

Jitka MOHYLOVA, Josef PUNCOCHAR, Stanislav ZAJACZEK

Department of Electrical Engineering, Faculty of Electrical Engineering and Computer Science, VSB–Technical University of Ostrava, 17. listopadu 15/2172, 708 33 Ostrava, Czech Republic

jitka.mohylova@vsb.cz, josef.puncochar@vsb.cz, stanislav.zajaczek@vsb.cz

DOI: 10.15598/aeee.v16i1.2317

Abstract. *This paper deals with application of simple synthetic inductor with series resistance (non-ideal gyrator). Those inductors are seldom used. However, if we use this inductor in the arm of bridge, the circuit is able to achieve high performance. In this way we can get band stop filter with good performance. In the paper we solve influence of real OPA properties. Theoretical considerations are verified by means of simulations (MicroCap) and experiments. Based on theoretical considerations, simulations and experiments are finally determined by criteria that must meet real operational amplifier to make the circuit performed well.*

Keywords

Band stop filter, frequency shift, minimum transmission, real OPA, synthetic inductor.

1. Introduction

In essence, the properties of an inductor can be simulated by a simple circuit with an amplifier called a synthetic inductor or gyrator. This basic circuit is presented in Fig. 1. The amplifier can be realized with vacuum tubes, transistors and integrated amplifying structures. This circuit is widely used for designing a band-stop and band pass filters. Although some authors (e.g. [2] and [3]) states: "The drawback of the circuit is that the quality factor is poor".

Nevertheless, this circuit (with an operational amplifier) is used to design the band-stop filter since 1971 [4], as shown in Fig. 2. The series resistance presented in Fig. 2, which is generally undesirable, is t functionally utilized in his circuit. This circuit has been described in literature [5], [6], [7] and [8] several times. However, it is necessary to describe the influence of the real synthetic inductor on the properties of the band-stop filter in detail (see Fig. 2).

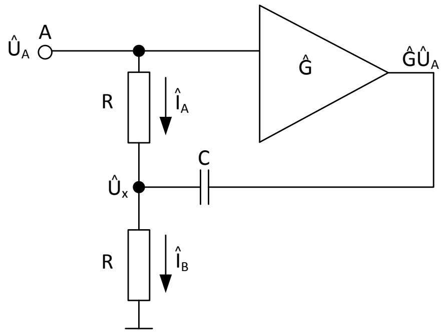

Fig. 1: Prescott gyrator.

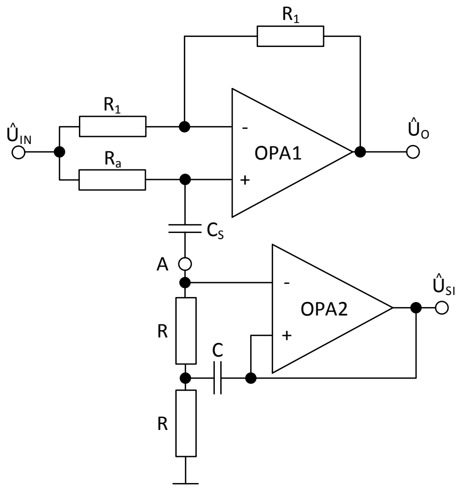

Fig. 2: Stop-band filter with synthetic inductor.

2. Prescott Inductor

Figure 1 shows the Prescott inductor (non-ideal gyrator). To find out the input impedance, current $\hat{I}_A$ and voltage $\hat{U}_X$ must be calculated by using superposition theorem. So we can come up with expressions:

$$\hat{U}_X = \frac{\hat{G}pCR + 1}{pCR + 2}, \tag{1}$$

where $p = j\omega$,

$$\hat{I}_A = \frac{\hat{U}_A - \hat{U}_X}{R} = \hat{U}_A \frac{pCR(1-\hat{G}) + 1}{2R + pCR^2}, \tag{2}$$

and input impedance

$$\hat{Z}_{IN} = \frac{\hat{U}_A}{\hat{I}_A} = \frac{2R + pCR^2}{1 + pCR(1-\hat{G})}. \tag{3}$$

If $\hat{G} = 1$, the expression for input impedance is described as:

$$\hat{Z}_{IN} = 2R + pCR^2. \tag{4}$$

Expression from Eq. (4) has been mentioned commonly in literature. The input impedance appears as a resistor R_S and inductor L connected in series. Where series resistor is defined as

$$R_S = 2R, \tag{5}$$

and inductor

$$L = CR^2. \tag{6}$$

If amplifier (follower) is realized with an operational amplifier, it follows that

$$\hat{G} = \frac{\hat{A}}{1 + \hat{A}}, \tag{7}$$

where $\hat{A}$ is the gain of the operational amplifier without feedback. Assuming that operational amplifier is well compensated and its gain is sufficiently described by the frequency of the first order model (e.g. [9] and [10]), we obtain:

$$\hat{A} = \frac{A_0\omega_1}{p + \omega_1} = \frac{\omega_T}{p + \omega_1}, \tag{8}$$

where ω_1 is the dominant (first) pole of transmission, ω_T is the extrapolated transition frequency ($\omega_T = A_0\omega_1$), and A_0 is the gain (DC) for $\omega < \omega_1$.

Further, we assume that that $\omega > \omega_1$ and normal operating mode of an operational amplifier while the normal values for ω_1 range from $2\pi \cdot 5$ rad·s^{-1} to $2\pi \cdot 50$ rad·s^{-1}. Then, the approximate relationship is valid when:

$$\hat{A} \approx \frac{\omega_T}{p}, \tag{9}$$

and

$$1 - \hat{G} = 1 - \frac{\hat{A}}{1 + \hat{A}} = \frac{1}{1 + \frac{\omega_T}{p}}. \tag{10}$$

When

$$\left|\frac{\omega_T}{p}\right| > 10, \tag{11}$$

then

$$1 - \hat{G} \approx \frac{p}{\omega_T}, \tag{12}$$

and by applying this formula to the Eq. (3), we get the following expression for input impedance

$$\hat{Z}_{IN} \approx \frac{2R + pCR^2}{1 + p^2\frac{CR}{\omega_T}}. \tag{13}$$

Real series R_{SR} resistance under these conditions is now frequency dependent and determined by the relation

$$R_{SR} = \frac{2R}{1 - \omega^2\frac{CR}{\omega_T}}, \tag{14}$$

as well as real inductor

$$L_R = \frac{CR^2}{1 - \omega^2\frac{CR}{\omega_T}}. \tag{15}$$

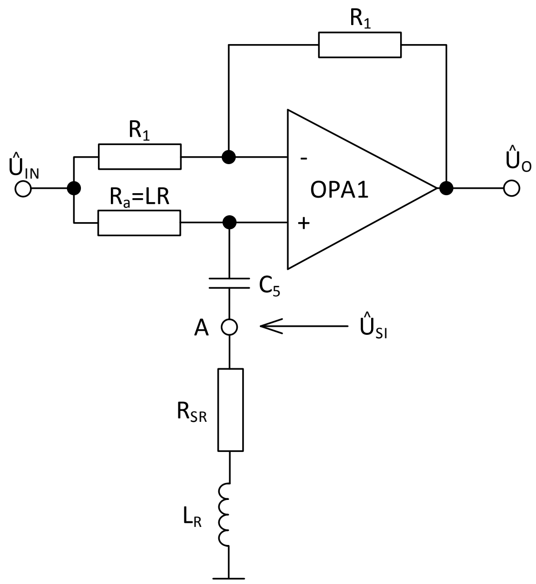

Fig. 3: Equivalent circuit of the circuit in Fig. 2.

3. Band Stop Filter with Synthetic Inductor

Fig. 3 shows equivalent circuit of the circuit in Fig. 2. If we make $R_a = 2R$, we can determine an expression relating $\hat{U}_{in}$ and $\hat{U}_{out}$ (so that we can find the gain) by the following expression:

$$\frac{\hat{U}_0}{\hat{U}_{IN}} = \frac{p^2 L_R C_S + pC_S(R_{SR} - 2R) + 1}{p^2 L_R C_S + pC_S(R_S R + 2R) + 1}. \tag{16}$$

If the operational amplifier op-amp2 is ideal ($\omega_T \to \infty$), then $R_{SR} = 2R$ and $L_R = CR^2$. At resonance (ideal state):

$$\frac{1}{j\omega_0 C_S} + j\omega_0 L = 0. \tag{17}$$

Therefore

$$\omega_0^2 = \frac{1}{LC_S} = \frac{1}{C_S C R^2}. \tag{18}$$

A quality factor Q is determined as follows

$$Q = \frac{\omega_0 L}{4R} = 0.25\sqrt{\frac{C}{C_S}}. \tag{19}$$

For frequency ω_0 is input of operational amplifier OP-AMP1 connected to a "balanced bridge $R_1 - R_1$; $2R - 2R$" and ideally $\hat{U}(\omega_0) \to 0$.

By modifying Eq. (18) and Eq. (19) we obtain the relationships suitable for design of the ideal circuit:

$$C_S = \frac{1}{4R\omega_0 Q}. \tag{20}$$

$$C = \frac{4Q}{R\omega_0}. \tag{21}$$

Simply, we select R and then use the above relationships. The bandwidth B is determined by elemental expression

$$B = \frac{\omega_0}{Q} = \frac{4}{RC}. \tag{22}$$

When varying ω_0 by means of C_S, B remains constant, whereas Q varies.

A more complex situation occurs when op-amp OP-AMP2 is non-ideal (and $\omega_0 > \omega_1$), then

$$\frac{1}{j\omega_r C_s} + j\omega_r L_R = 0. \tag{23}$$

By solving this equation, we get

$$\omega_r^2 = \omega_0^2 \frac{1}{1 + \dfrac{1}{\omega_T R C_S}}. \tag{24}$$

Resulting expression for series resistor R_{SR} at frequency ω_r using Eq. (24) is determined as:

$$R_{SR} = \frac{2R}{1 - \dfrac{\omega_r^2}{\omega_T C R}} - \frac{2R}{1 - \dfrac{1}{1 + RC_S\omega_T}}. \tag{25}$$

This means that the operational amplifier OP-AMP1 (for $R_a = 2R$) at frequency ω_r is not balanced and transmission is different from zero. From Eq. (16), it is evident that

$$T_{\min} = \left.\frac{\hat{U}_0}{\hat{U}_{IN}}\right|_{\omega_r} = \frac{R_{SR} - 2R}{R_{SR} + 2R} \neq 0. \tag{26}$$

Substituting for R_{SR} from Eq. (25) into Eq. (26) we get after modifications (for $R_a = 2R$ - see Fig. 3):

$$T_{\min} = \left.\frac{\hat{U}_0}{\hat{U}_{IN}}\right|_{\omega_r} = \frac{1}{1 + 2\omega_T R C_S}. \tag{27}$$

4. Maximum Input Voltage

The results of the experiments showed that the amplitude of the input voltage is limited by the output of OP-AMP2. If the voltage $\hat{U}_{SI}$ is limited, we cannot use a linear model, which has always been used.

Using the assumption that the operational amplifier is ideal, we get:

$$\begin{aligned} &\hat{U}_{SI} = \hat{U}_A = \hat{U}_{IN} \frac{2R + pCR^2}{2R + \dfrac{1}{pC_S} + 2R + pcR^2} \Rightarrow \\ &\Rightarrow \frac{\hat{U}_{SI}}{\hat{U}_{IN}} = \frac{p^2 C_S C R^2}{p^2 C_S C R^2 + p4RC_S + 1} + \\ &+ \frac{p^2 C_S R}{p^2 C_s C R^2 + p4RC_S + 1}. \end{aligned} \tag{28}$$

By analysing Eq. (28) it was found that the maximum allowable amplitude for the input signal is

$$U_{IN\,\max} \cong \frac{\min(|U_{CC-}|, U_{CC+} - 2\mathrm{V})}{\sqrt{0.25 + Q^2}}, \tag{29}$$

where U_{CC-}, U_{CC+} define the value of the supply voltage, Q is the quality factor (Eq. (19)) [6].

5. Real Quality Factor of Band Stop Filter

The above considerations are concerning the exact resonant frequency ω_r. However, by substituting L_R and R_{SR} in Eq. (16) for transfer function we obtain relationship from which it is not possible to determine the bandwidth B (change of 3 dB), see [11]. Simulation results from [11] are briefly summarized in Tab. 1. The results in Tab. 1 shows how the ratio Q_r/Q is dependent on an expression $\omega_T/(Q\omega_0)$, see below. From data in Tab. 1 it is evident that for the real values of $\omega_T/(Q \cdot \omega_0)$, the changes of Q_r are already insignificant The ideal state corresponds to $\omega_T/(Q \cdot \omega_0) \to \infty$.

Tab. 1: Change Q_r/Q dependent on $\omega_T/(Q\omega_0)$.

$\frac{\omega_T}{Q\cdot\omega_0}$	$\frac{Q_R}{Q}$
(-)	(-)
10	1.42
20	1.22
50	1.10
100	1.07

6. Verification of Theoretical Considerations

To verify theoretically derived relationship, a number of simulations and measurements under various conditions has been carried out. It turned out that it is necessary to modify the obtained relations into an appropriate (normalized) form. For this reason, the product of $\omega_T RC_s$ was modified as follows:

$$\omega_T RC_S = \omega_T R\sqrt{C_S}\sqrt{C_S} = \\ = \omega_T R\sqrt{C_S}\sqrt{C_S}\cdot\frac{\sqrt{C}}{\sqrt{C}} = \omega_T R\sqrt{CC_S}\cdot\frac{\sqrt{C_C}}{\sqrt{C}}, \tag{30}$$

thus

$$\omega_T RC_S = \frac{\omega_T}{\omega_0}\cdot\frac{1}{\sqrt{\frac{C}{C_S}}} = \\ = \left| Q = \frac{\sqrt{\frac{C}{C_S}}}{4} \right| = \frac{\omega_T}{4Q\omega_0}. \tag{31}$$

Then

$$\left(\frac{\omega_r}{\omega_0}\right)^2 = \frac{1}{1+\frac{1}{\omega_T RC_S}} = \\ = \frac{1}{1+4\frac{Q\omega_0}{\omega_T}} = \frac{1}{1+4\frac{Qf_0}{f_T}}, \tag{32}$$

$$\frac{R_{SR}}{2R} = \frac{1}{1-\frac{1}{\omega_T RC_S+1}} = \\ = \frac{1}{1-\frac{4\frac{Q\omega_0}{\omega_T}}{1+4\frac{Q\omega_0}{\omega_T}}} = \frac{1}{1-\frac{4\frac{Qf_0}{f_T}}{1+4\frac{Qf_0}{f_T}}}, \tag{33}$$

$$\left.\frac{\hat{U}_0}{\hat{U}_{IN}}\right|_{\omega_r} = T_{\min} = \frac{1}{1+2\omega_T RC_S} = \\ = \frac{1}{1+0.5\frac{\omega_T}{Q\omega_0}}. \tag{34}$$

It is apparent that the ratio $\omega_T/(Q\omega_0)$ is important. For $\omega_T/(Q\cdot\omega_0)\to\infty$, we obtain the ideal value 1 or zero.

Simulations were performed in a Microcap software. For the simulations, we used resistors $R_1 = 10$ kΩ, $R = 5$ kΩ, the capacity C_s ranged from 80 pF to 80 nF, the capacity C ranged from 128 nF to 1280 nF; the transition frequency f_T of operational amplifiers ranged from 50 kHz to 10 MHz (see Fig. 2). The frequency of the op amp second pole has always been shifted, thus was higher than the frequency f_T. It turned out that the properties of the operational amplifier op-amp1 practically do not affect (ω_r/ω_0) and $T_{\min}$, if $(\omega_T/\omega_0) > 10$. This obviously affects the overall transfer function since the decrease of transmission op-amp1 by 3 dB, under these conditions, is at a frequency $\omega_T/2$. Equation (16) can be adjusted into

$$\frac{\hat{U}_0}{\hat{U}_{IN}} = \frac{p^2 L_R C_S + pC_S(R_{SR}-2R)+1}{p^2 L_R C_S + pC_S(R_{SR}+2R)+1}\cdot\frac{\frac{\omega_T}{2}}{p+\frac{\omega_T}{2}}. \tag{35}$$

Table 2 summarizes the results obtained experimentally in comparison with the ideal values calculated using Eq. (32) and Eq. (34). Values $\omega_T/(Q\omega_0)$ were obtained by different combinations of ω_T, Q, and ω_0. It was confirmed that the result of the product is decisive in comparison with the individual expressions in the normalized form.

Tab. 2: Results of simulation ($R_a = 2R$) and calculations for the circuit of Fig. 2 according to the ratio $\omega_T/(Q\cdot\omega_0)$.

$\frac{\omega_T}{Q\cdot\omega_0}$	**Simulation**		Eq. (32)	Eq. (34)
	$\frac{f_r}{f_0}$	$T_{\min}$	$\frac{f_r}{f_0}$	$T_{\min}$
$(-)$	(-)	(dB)	(-)	(dB)
10.05	0.8459	-15	0.8458	-15.6
25.13	0.9287	-22	0.9288	-22.6
50.26	0.9623	-28	0.9624	-28.3
100.5	0.9806	-34	0.9807	-34.2
251.3	0.9920	-42	0.9920	-42.0
502.7	0.9961	-48	0.9960	-48.0
1005	0.9981	-55	0.9980	-54.0
3351	0.9995	-63	0.9994	-64.5
10531	0.99978	-73	0.9998	-74.3

Although Eq. (33) is explicitly verified by the relationship Eq. (34), we have verified simulations for several values of $R_{SR}/(2R)$ and these results are shown in Tab. 3. Simulations were carried out under similar conditions as in previous case (see Tab. 3). The difference lies in the fact that the second pole of the response

Tab. 3: Results of simulation ($R_a = 2R$) and calculations for the circuit of Fig. 2 according to the ratio $\omega_T/(Q\cdot\omega_0)$.

f_T	$\frac{f_r}{Q\cdot f_0}$	**Simulation**		Eq. (32)	Eq. (33)
		$\frac{f_r}{f_0}$	$\frac{R_{SR}}{2R}$	$\frac{f_r}{f_0}$	$\frac{R_{SR}}{2R}$
(MHz)	(-)	(-)	(-)	(-)	(-)
0.6	181	0.98895	1.0262	0.98913	1.0221
1.0	302	0.99333	1.0171	0.99344	1.0133
2.0	604	0.99666	1.0105	0.99671	1.0066
10.0	3016	0.99932	1.0049	0.99934	1.0013

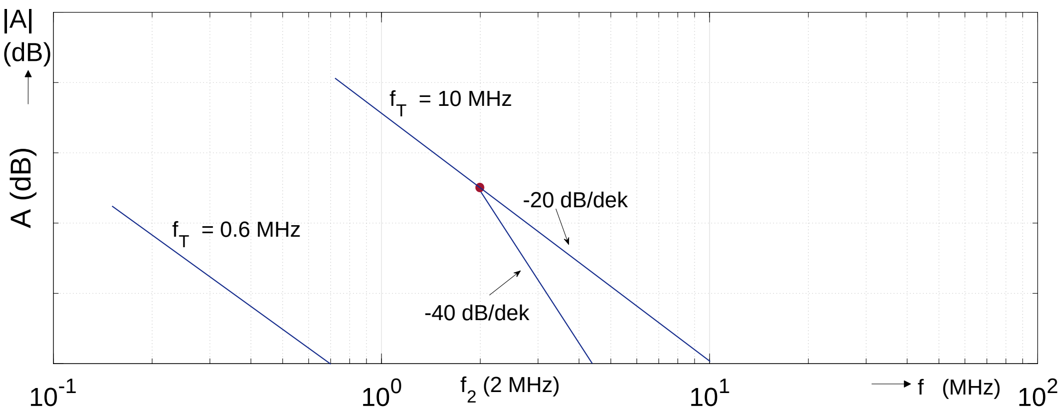

Fig. 4: Quantitative representation of the transmission of the operational amplifier at a fixed position of the second pole f_2.

Tab. 4: Results of the simulations [11] and calculations according to equations Eq. (32) and Eq. (34); quality factor Q_r - determined by means of simulation.

OZ	f_r	$\frac{f_r}{Q \cdot f_0}$	**Simulation** [11]			Eq. (32)	Eq. (34)
			$\frac{f_r}{f_0}$	Q_r	$T_{\min}$	$\frac{f_r}{f_0}$	$T_{\min}$
	(MHz)	(-)	(-)	(-)	(dB)	(-)	(dB)
µA741	≈ 1	6.2877	0.7600	2.77	-12	0.7818	-12.35
LF351	≈ 4	25.1508	0.9209	1.91	-22	0.9289	-22.65
LF400	≈ 18	113.18	0.9805	1.65	-35	0.9828	-35.20

curve of the operational amplifier op-amp2 was fixed to 2 MHz.

It is obvious that the position of the second operational amplifier pole (op-amp2, f_2) substantially affects primarily the value of R_{SR}, especially when transmission on f_2 "emerges over 0 dB (here for $f_T > 1$ MHz) as shown in Fig. 4. The ratio f_r/f_0 remained practically unchanged.

In [11], the simulations were carried out for three different real operational amplifiers, see Fig. 5.

Ideally, the desired frequency $f_0 = 100.658$ kHz and $Q = 1.58$. The results of the simulations and calculations are summarized in Tab. 4.

The simulations show that the derived relationships describe the behaviour of the circuit at the retention frequency precisely.

Derived relations were verified by measurements. The circuit of the band stop filter was realized according to Fig. 2. This circuit was consisted of the following components: resistor values $R_1 = 15$ kΩ (twice), $R_a = 2 \cdot 15$ kΩ, $R = 15$ kΩ (twice) - resistors with an accuracy of one percent, the capacitance value $C = 1$ µF, operational amplifiers op-amp1 and op-amp2 - both µA741, power supply ± 12 V. The amplitude of the input voltage is 1.41 V. Assume $f_T = 1$ MHz. The results of measurement and calculation for different values of C_S are summarized in Tab. 5 and Tab. 6.

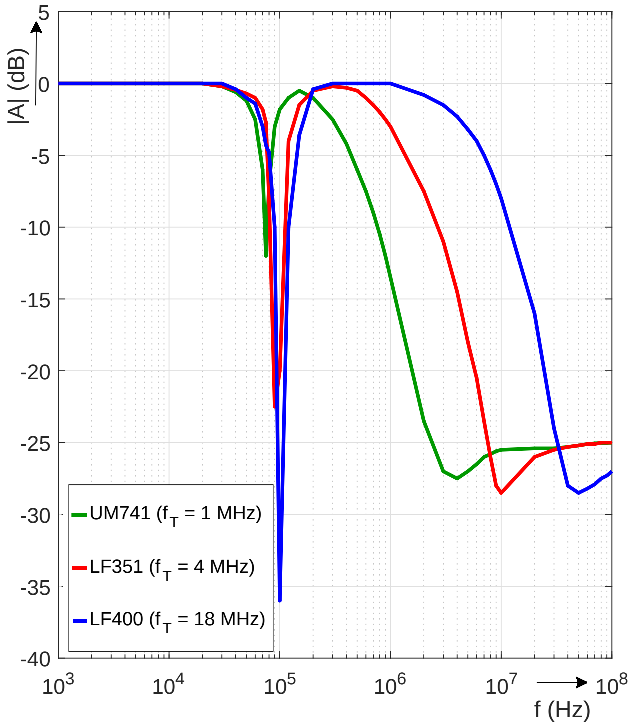

Fig. 5: Simulation of properties band-stop filter according to Fig. 2, three different operational amplifiers.

For the given $f_T/(Qf_0)$, the measured values (f_r/f_0) are determined only accuracy of passive elements". The same statement applies to the minimum transmission $T_{\min}$. If the resistance tolerance is 1 %, the actual resistance value R_a can be, for example, up to 30 kΩ + 300 Ω and thus the actual value of the resistor $R_S = 2R$ may be up to 30 kΩ − 300 Ω.

By substituting these values into Eq. (26) [$R_S \rightarrow$ 30 kΩ −300 Ω; $2R \rightarrow$ 30 kΩ +300 Ω] we obtain:

$$T_{\min} = \frac{30 \cdot 10^3 - 300 - 30 \cdot 10^3 - 300}{30 \cdot 10^3 - 300 + 30 \cdot 10^3 + 300} = \\ = \frac{-600}{60 \cdot 10^3} = -10^{-2}. \tag{36}$$

This corresponds to transmission (at f_r) −40 dB. The value of $T_{\min}$ is determined by accuracy of resistors not by properties of the operational amplifier op-amp2. The non-optimal op-amp (described f_T/Qf_0) then increases the value of $T_{\min}$, but the trend remains, i.e. the lower the ratio $f_T/(Qf_0)$, the higher the $T_{\min}$.

Tab. 5: Calculated values for the circuit of Fig. 2 under the conditions described in the text.

C_S	Calculation				
	Eq. (18)	Eq. (19)	–	Eq. (32)	Eq. (34)
	f_0	Q	$\frac{f_r}{Q \cdot f_0}$	$\frac{f_r}{f_0}$	$T_{\min}$
(nF)	(Hz)	(-)	(-)	(-)	(dB)
1.0	335.5	7.91	376.98	0.9938	−45.6
2.2	226.2	5.33	829.35	0.9976	−52.4
3.3	184.7	4.35	1244.1	0.9984	−55.9
5.4	144.4	3.40	2037.0	0.9990	−60.2
82	37.05	0.87	30916	$\rightarrow 1$	−83.8

Tab. 6: Measured values for the circuit of Fig. 2 for the conditions described in the text. Note 1 - The big difference measured and calculated values of quality factor.

C_S	Measurement					
	f_0	Q_r	$\frac{f_r}{f_0}$	$T_{\min}$	B	**Note**
(nF)	(Hz)	(-)	(-)	(-)	(Hz)	
1.0	335.5	2.80	0.9597	−27.0	115	1
2.2	226.2	5.2	0.9460	−30.5	41	
3.3	184.7	4.3	0.9637	−32.6	41	
5.4	144.4	3.4	0.9557	−40.0	40	
82	37.05	0.9	0.9459	−41.6	39	

According to [5], when setting the minimum transition T_{MIN} (at f_0) it is possible to set the resistance value R_a individually for each set frequency f_0 (f_r) so that the transition $T_{\min}$ is less than −40 dB. Practically useful circuit connection is achieved by changing the resistance R_a by a serial combination of trimmer and fixed resistance (see Fig. 2). Our experiments used a combination of 27 kΩ and a 6.8 kΩ resistors. Again, it was always possible to set a transition $T_{\min}$ less than −45 dB without changing the frequency. This setting compensates the actual operational amplifier properties and the final tolerance of the resistors at the same time (of course, this problem is not the case with simulations since the resistor values are set precisely).

We must pay attention to the required value of $Q = 7.91$ (see $C_s = 1$ nF in Tab. 5). Detailed measurements (for the conditions in Tab. 5) are shown in Tab. 7 for the amplitude of the input signal $U_{IN\ A} = 1.41$ V (i.e. effective value 1 V). In addition to the output voltage $\hat{U}_0$, the voltage at the output op-amp2 ($\hat{U}_{SI}$), which is defined by Eq. (28), is measured. At the required value of $Q = 7.91$, a significant resonance maximum is achieved, resulting in a limitation of the voltage at the op-amp2 output (at ±12 V supply). The circuit is "non linear" for $U_{IN} = 1.41$ V and this leads to degradation of its properties.

If the power supply voltage is increased to 15 V, the $\left|\hat{U}_{SI}/\hat{U}_{IN}\right|$ ratio at 310 Hz is equal to 7.167 (17.11 dB) and at 321 Hz at 7.50 (17.50 dB) with the amplitude $U_{SI\ A} = 10.58$ V. The quality factor Q was returned to 7.8, the value $T_{\min}$ is −28.6 dB (at 322 Hz), while the influence of inaccurate (real) resistors is still applied here. We will achieve the same effect by lowering the amplitude $U_{IN\ A}$ below 1.2 V. The maximal input voltage is determined by substituting Q in Eq. (29):

$$U_{CC} = \pm 12\,\mathrm{V} \Rightarrow U_{IN\max} \cong \\ \cong \frac{12 - 2}{\sqrt{0.25 + 7.905^2}} = 1.262\ \mathrm{V}. \tag{37}$$

$$U_{CC} = \pm 15\,\mathrm{V} \Rightarrow U_{IN\max} \cong \\ \cong \frac{15 - 2}{\sqrt{0.25 + 7.905^2}} = 1.641\ \mathrm{V}. \tag{38}$$

For comparison, of a circuit with a lower quality factor ($Q = 3.40$) was measured (see in Tab. 5 - $C_S = 5.4$ nF), again for ±12 V supply, $R_a = 2R$; $U_{IN\ A} = 1.41$ V. Now

$$U_{IN\max} \cong \frac{12 - 2}{\sqrt{0.25 + 3.40^2}} = 2.91\ \mathrm{V}. \tag{39}$$

The circuit will still work in linear mode, see Tab. 8.

In both cases, harmonic distortion was observed for frequencies higher than 40 kHz (amplitude of 1.41 V). This is a slew rate distortion where the power frequency f_p is defined by the following relationship (see for instance [10]):

$$f_p = \frac{SR}{2\pi U_A}, \tag{40}$$

where SR is the slew rate (V·s^{-1}), U_A is the amplitude of signal.

For operational amplifier µA741, a typical slew rate $SR = 0.5$ V·µs^{-1} $= 5 \cdot 10^5$ V·s^{-1} is given. Assuming that $U_A = 1.41$ V, the power frequency f_p becomes

$$f_p = \frac{5 \cdot 10^5}{2\pi \cdot 1.41} = 56.44\ \mathrm{kHz}. \tag{41}$$

Therefore it can be assumed that the actual value of the slew rate is lower. If the threshold frequency is

Tab. 7: The measurement of band stop filter for amplitude $U_{IN\ A} = 1.41$ V, $U_{SI\ A}$ - the amplitude of the voltage at the op-amp2 output (at ± 12 V supply); $R_a = 2R$; $C_S = 1$ nF, $Q = 7.91$.

f	$\left\|\frac{\hat{U}_0}{\hat{U}_{IN}}\right\|$	$\left\|\frac{\hat{U}_{SI}}{\hat{U}_{IN}}\right\|$	$\left\|\frac{\hat{U}_{SI}}{\hat{U}_{IN}}\right\|$	$U_{SI\ A}$	**Note**
Hz	(dB)	(-)	(dB)	(V)	
10	0	$3.3 \cdot 10^{-3}$	-49.6	$4.46 \cdot 10^{-3}$	-
80	-0.40	0.072	-22.9	0.102	-
200	-1.94	0.667	-3.52	0.94	-
270	-3.31	2.530	8.06	3.57	-
300	-5.46	5.667	15.1	7.99	-
310	-8.33	6.667	16.5	9.40	limitation
321	-25.8	6.667	16.5	9.40	limitation
322	-26.9	6.667	16.5	9.40	limitation
323	-25.9	6.667	16.5	9.40	limitation
324	-23.5	6.610	16.4	9.32	-
330	-13.3	6.500	16.26	9.17	-
380	-4.21	3.067	9.73	4.32	-
1000	0	1.133	1.08	1.60	-
$4 \cdot 10^4$	-0.15	0.983	-0.15	1.31	distortion
10^5	-1.94	0.667	-3.38	0.94	distortion

Tab. 8: The measurement of band stop filter for amplitude $U_{IN\ A} = 1.41$ V, supply $= \pm 12$ V; $R_a = 2R$; $C_S = 5.4$ nF, $Q = 3.4$.

f	$\left\|\frac{\hat{U}_0}{\hat{U}_{IN}}\right\|$	$\left\|\frac{\hat{U}_{SI}}{\hat{U}_{IN}}\right\|$	$\left\|\frac{\hat{U}_{SI}}{\hat{U}_{IN}}\right\|$	$U_{SI\ A}$	**Note**
(Hz)	(dB)	(-)	(dB)	(V)	
10	0	0.012	-38.7	$17 \cdot 10^{-3}$	-
60	0	0.250	-12.0	0.353	-
80	-0.17	0.517	-5.74	0.729	-
100	-0.76	1.100	0.83	1.551	-
110	-1.80	1.533	3.71	2.161	-
120	-3.10	2.267	7.11	3.196	-
130	-8.33	3.067	9.73	4.324	-
137	-24.4	-	-	-	-
138	-40.0	-	-	-	-
140	-21.0	3.533	10.96	4.982	-
150	-6.32	3.333	10.46	4.700	-
160	-3.10	2.867	9.15	4.042	-
180	-0.92	2.129	6.56	3.002	-
200	-0.15	1.129	1.05	1.592	-
1000	-0.07	1.016	0.14	1.432	-
10^4	-0.07	1.016	0.14	1.432	-
$4 \cdot 10^4$	-0.15	0.968	-0.28	1.365	distortion
10^5	-1.94	0.667	-3.38	0.940	distortion

$f_p = 40$ kHz, then the slew rate is defined as:

$$\begin{aligned} SR &= f_p \cdot 2\pi U_A = \\ &= 35.437\ \mathrm{V \cdot s^{-1}} = 0.354\ \mathrm{V \cdot \mu s^{-1}}. \end{aligned} \tag{42}$$

When verifying SR using a rectangular input signal, this value is actually confirmed.

7. Summary

The degradation of the operational amplifier properties (especially op-amp2) leads to change of a resonant frequency and to relatively high value $T_{\min}$ transmissions at this frequency. However, the $T_{\min}$ value can be easily reduced in the practical circuit by setting the resistance value R_a, see Fig. 6. Many simulations and practical measurements have verified the Eq. (32), Eq. (33) and Eq. (34) when the gain on the second pole of the op-amp2 is less than 0 dB.

From the equation Eq. (32), the desired size of ratio $[f_T/f_0Q]k$ can be derived by means of elementary adjustments to achieve $f_r = kf_0$ (ideally $k = 1$):

$$\frac{f_T}{f_0Q}_k = \frac{4}{\left(\frac{f_0}{f_r}\right)^2 - 1} = |f_r = kf_0| = \frac{4k^2}{1-k^2}. \tag{43}$$

for

$$k = 0.99 \Rightarrow \left(\frac{f_T}{f_0Q}\right)_{k=0.99} = 197. \tag{44}$$

$$k = 0.95 \Rightarrow \left(\frac{f_T}{f_0Q}\right)_{k=0.95} = 41. \tag{45}$$

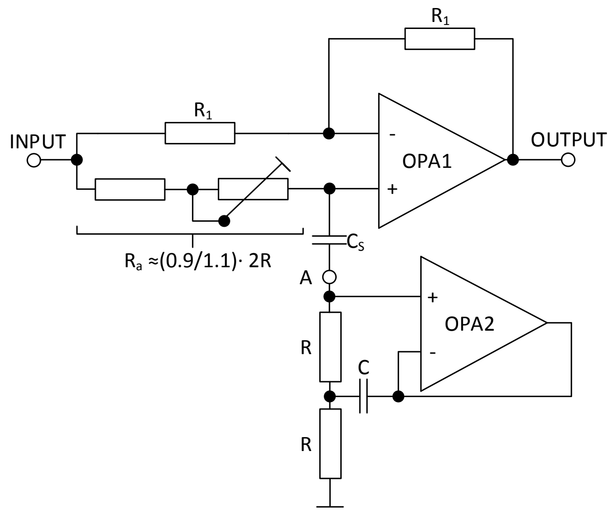

Fig. 6: Modifying R_a for setting minimum value $T_{\min}$.

From Eq. (34), the desired $[f_T/f_0Q]$ for $T_{\min}$ can be determined (at $R_a = 2R$):

$$\left(\frac{f_T}{f_0Q}\right) = \left(\frac{1}{T_{\min} - 1}\right) \cdot 2, \qquad (46)$$

$$T_{\min} = 0.1(-20\,\mathrm{dB}) \Rightarrow \left(\frac{f_T}{f_0Q}\right)_{T_{\min}=0.1} = 18, \qquad (47)$$

$$T_{\min} = 0.5(-26\,\mathrm{dB}) \Rightarrow \left(\frac{f_T}{f_0Q}\right)_{T_{\min}=0.05} = 38, \qquad (48)$$

$$T_{\min} = 0.01(-40\,\mathrm{dB}) \Rightarrow \left(\frac{f_T}{f_0Q}\right)_{T_{\min}=0.01} = 198. \qquad (49)$$

It is obvious that for practical use it is advisable to provide f_T/f_0Q greater than 200.

8. Conclusion

Although circuits of this type (such as the one showed in Fig. 2) have already been investigated, the article brings new results that allow to design a band stop filter according to real properties. From Sec. 7. it is clear that the circuit will be suitable for relatively low f_0 values, for example in medical applications

Acknowledgment

This article was supported by SP2017/152 "Vyzkum antennich systemu, diagnostika a spolehlivost elektrickych stroju a zarizeni". The authors acknowledge for support.

References

[1] PRESCOTT, A. J. Loss-compensated active gyrator using differential-input operational amplifiers. *Electronics Letters*. 1966, vol. 2, no. 7, pp. 283–284. ISSN 0013-5194. DOI: 10.1049/el:19660239.

[2] JAYALALITHA, D. S. and D. SUSAN. Grounded Simulated Inductor - A Review. *Middle-East Journal of Scientific Research*. 2013, vol. 15, no. 2, pp. 278–286. ISSN 1990-9233. DOI: 10.5829/idosi.mejsr.2013.15.2.3706.

[3] KUMAR, U., S. K. SHUKLA and AMIETE. Analytical Study of Inductor Simulation Circuits. *Active and Passive Electronic Components*. 1989, vol. 13, iss. 4, pp. 211–227. ISSN 1563-5031. DOI: 10.1155/1989/39762.

[4] *The Linear Integrated Circuits Data Catalog: Notch filter using the µA741 as a gyrator*. 1st ed. Mountain View: Fairchild Semiconductor Components Group Fairchild Camera and Instrument Corporation, 1971.

[5] PUNCOCHAR, J. Pasmova zadrz se syntetickou indukcnosti. *Sdelovaci technika*. 1984, vol. 32, no. 2, pp. 49–51. ISSN 0036-9942.

[6] PUNCOCHAR, J. Maximalni vstupni napeti pro zadrze RC. *Sdelovaci technika*. 1980, vol. 28, no. 10, pp. 365–366. ISSN 0036-9942.

[7] PUNCOCHAR, J. Zapojeni nizkofrekvencniho zesilovace s nastavitelnou frekvencni charakteristikou. *Sdelovaci technika*. 1984, vol. 32, no. 9, pp. 331–333. ISSN 0036-9942.

[8] PUNCOCHAR, J. Narrow band-reject filter with real operational amplifier. In: *10th International Czech-Slovak Scientific Conference Radioelektronika*. Bratislava: Slovak University of Technology in Bratislava, 2000, pp. 1–3. ISBN 80-227-1389-9.

[9] PUNCOCHAR, J. *Operacni zesilovace v elektronice*. 1st ed. Prague: BEN, 2002. ISBN 80-730-0059-8.

[10] MOHYLOVA, J. and J. PUNCOCHAR. *Theory of electronic circuits*. 1st ed. Ostrava: VSB–Technical University of Ostrava, 2013. ISBN 978-80-248-3112-1.

[11] KOLAR, J. *Realne operacni site typu pasmova zadrz*. Ostrava, 2007. Master thesis. VSB–Technical University of Ostrava. Supervisor Josef Puncochar.

[12] PRUTCHI, D. and M. NORRIS. *Design and Development of Medical Electronic Instrumentation:*

A Practical Perspective of the Design, Construction, and Test of Medical Devices. 1st ed. New Jersey: John Wiley & Sons, 2005. ISBN 0-471-67623-3.

About Authors

Jitka MOHYLOVA was born in Opava, Czech Republic in 1959. In 1983 she graduated in radioengineering - biomedical engineering from VUT FE Brno. She received the Ph.D. degree in cybernetics from the Faculty of Electrical Engineering and Computer Science, VSB–Technical University Ostrava in 2002. Since 1990 she has been with Faculty of Electrical Engineering and Computer Science, VSB–Technical University Ostrava, where she is now Assistent Professor at Department of Electrotechnics. Her present interests are in the circuit theory, theoretical and experimental electronics, e.g. the influence of real properties of an op amp on the behaviour of filters and biomedical signal processing.

Josef PUNCOCHAR was born in Dolni Vestonice, Czech Republic in 1948. In 1971 he graduated in radioengineering from VUT FE Brno. He received the Dr. degree in electronics from the Faculty of Electrical Engineering and Computer Science, VSB–Technical University Ostrava in 1996. From 1971 to 1992 he was with TESLA Roznov (measurement and application of linear integrated circuits). Since 1992 he has been with Faculty of Electrical Engineering and Computer Science, VSB–Technical University Ostrava, where he is now Associate Professor at Department of Electrotechnics. His present interests are in the circuit theory, theoretical and experimental electronics, e.g. the influence of real properties of an op amp on the behaviour of filters.

Stanislav ZAJACZEK was born in 1978 in Havirov. He graduated at the department of electrical machinery and apparatus at the Technical University of Ostrava. Since 2006 he has been with of Electrical Engineering and Computer Science, VSB–Technical University Ostrava, he is now Assistant Professor at Department of Electrical Engineering. In 2010 he earned his Ph.D. In the scientific field deals with the shape optimization.